

A Comparative Study on Automatic Flight Control for small UAV

Elfatih A. Hamdi, Gamal M. Sayed El-Bayoumi

Aeronautical Engineering Department, Engineering College, Cairo University
Giza State, Egypt
elfatihguma@gmail.com; gelbayoumi@yahoo.com

Abstract - The UAV flight control system is rich with attractive and challenging design problems to achieve robust stability and acceptable performance level across specified flight envelope in the presence of uncertainties. Therefore, this paper is devoted to design an adequate flight control system for stabilizing a fixed wing (**Aerosonde**) UAV under exogenous inputs. In order to guarantee the stability of the closed loop system while maintaining some acceptable level of performance, the controller is designed using H_∞ loop-shaping design procedure (LSDP) which is one of the robust control techniques first. Then, the designed robust controller is compared with classical controller which was designed in a previous work for the same aircraft dynamic. The comparison is performed in terms of performance specifications, and in terms of robust stability requirements which include disturbance rejection, noise attenuation, unmodeled dynamics, and control effort. The obtained results clarify the ability of the designed controller using robust technique to cope with the specified levels of uncertainty in addition to its superior capabilities upon the classical technique.

Keywords: UAV, Flight Control, Robust Control, Classical Control.

1. Introduction

The H_∞ loop-shaping design procedure (LSDP) is a sensible and powerful procedure combined with the classical loop shaping of the open loop system frequency response to have a desired loop shape. It is a part of the H-infinity optimization problem that has been developed by McFarlane and Glover. The feature of this technique is that the closed loop requirements (disturbance rejection and noise attenuation properties) can be specified by shaping the open-loop gains. The obtained controller is robust against the normalized coprime factor uncertainty. Whenever the LSDP is used, the optimal robust controller can be limited to solve two Riccati equations [1]; (Control Algebraic Riccati Equation (CARE) and Filter Algebraic Riccati Equation (FARE)). Thus, the robust stabilization problem reduces to the solution of the two Riccati equations simultaneously instead of γ -iteration process associated with traditional loop shaping such as mixed-sensitivity [1].

2. Uncertainty Representation

For the LSDP, the coprime factor uncertainty is considered. In this description, an unstable transfer function can be represented by two stable coprime factors, figure (1), which contains no unstable hidden modes. If we considered a perturbation about G (nominal transfer function) then the perturbed transfer function can written as:

$$G_\Delta = \frac{N + \Delta_N}{M + \Delta_M} \quad (1)$$

Where Δ_N and Δ_M are unknown stable real-rational transfer functions.

Two of H_∞ loop shaping design procedures (LSDP) are available which can be explained in the following sections.

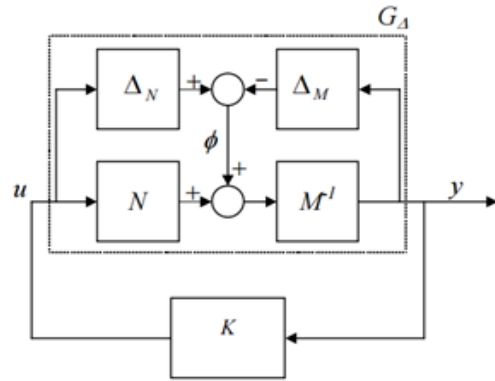


Fig. 1: Normalized left coprime factor uncertainty description.

3. Trial and Error Method

A LSDP is basically, two stages design procedures. In the first stage the original open-loop system, G is shaped by the two shaping functions, W_1 (pre-compensator) and W_2 (post-compensator), figure (1), to match as closely as possible a desired shape of the open-loop frequency response. The shaped plant is formulated as normalized coprime which separates the plant G_s into normalized nominator N_s and denominator M_s factors figure (1):

$$G_s = W_1 G_\Delta W_2 = \begin{bmatrix} A_s & B_s \\ C_s & D_s \end{bmatrix} = \frac{N_s + \Delta_s}{M_s + \Delta_s} \quad (2)$$

Then, in the second stage, the controller is formed by combining the central controller K_∞ with the shaping functions W_1 and W_2 as shown in the figure (2). The final controller, figure(3), can be written as

$$G_s = W_1 K_\infty W_2 = \begin{bmatrix} A_k & B_k \\ C_k & D_k \end{bmatrix} \quad (3)$$

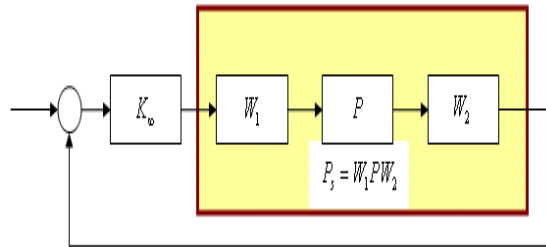


Fig. 2: P is shaped by W_1 and W_2 and stabilized by K_∞ .

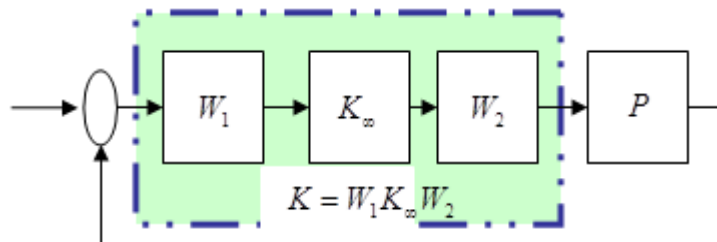


Fig. 3: Final controller K is constructed by combining K_∞ with W_1 and W_2 .

Here for this method the shaping functions W_1 and W_2 are computed manually and there is a certain rule to be followed.

4. Auto-Tune Method

This technique has been developed by Safonov-Le [2] for designing an optimal and stable minimum-phase Glover-McFarlane Pre-filter W . This locates (fitting) singular values of the open-loop frequency response to any desired location as precisely as possible. The algorithm combines a novel all-pass squaring-down compensator technique, of Safonov-Le, together with optimal Balanced Stochastic Truncation (BST) minimal realization techniques and normalized-coprime optimal H_∞ synthesis. Further, the Safonov-Le pre-filter has the important property that plant RHP zeros are left invariant; i.e., no performance-limiting RHP zeros and poles are introduced. The result is that the designer is completely relieved of task of manually computing the weight W . Designing an optimal loop shaping controller K for plant G with this algorithm is simple as specifying the desired loop shape G_d [2]. The block diagram of the shaped plant and controller can be shown in figures (4) and (5) respectively.

As previously stated in the section 2 the shaped plant and final robust controller can be formulated as in the equations (3) and (4) respectively.

$$G_s = WG = \begin{bmatrix} A_s & B_s \\ C_s & D_s \end{bmatrix} = \frac{N_s + \Delta_s}{M_s + \Delta_s} \quad (4)$$

$$K = K_\infty G = \begin{bmatrix} A_k & B_k \\ C_k & D_k \end{bmatrix} \quad (5)$$

Where W is the Safonov-Le filter

Here, in this paper, the target desired method was used to design the relevant controller that stabilizes the aircraft longitudinal dynamics against the different type of uncertainties.

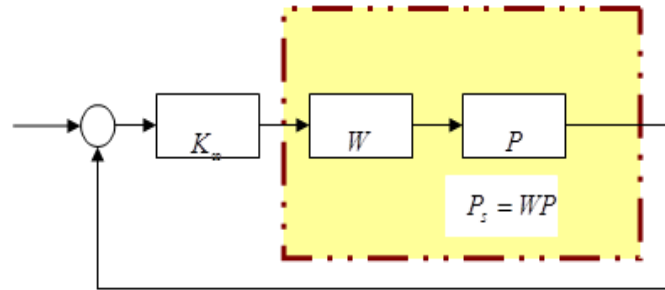


Fig. 4: P is shaped by W and stabilized by K_∞ .

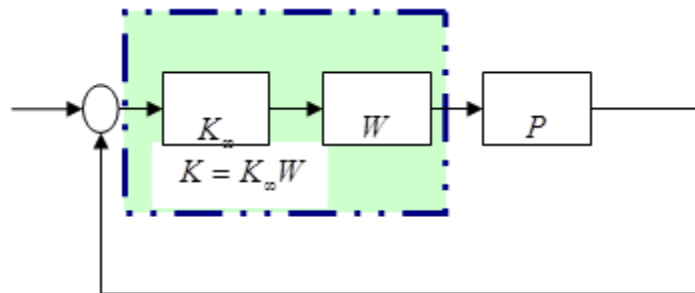


Fig. 5: Final controller K is constructed by combining K_∞ with W .

5. Problem Formulation

Given a shaped plant G_s , the robust stabilization problem is to find a realizable and stabilizable optimal robust controller K such that

$$\left\| \begin{bmatrix} K \\ I \end{bmatrix} (I - G_s K)^{-1} M^{-1} \right\|_{\infty} \leq \frac{1}{\varepsilon} = \gamma \quad (6)$$

where γ is the $\|H\|_{\infty}$ from \emptyset , to $[u \quad y]^T$, and $(I - G_s K)^{-1}$ is the sensitivity function. Mc-Farlane and Glover have shown that, if the normalized coprime uncertainty is used, the optimal values of ε or γ_{min} can be found directly without iteration from the following relation [3]:

$$\gamma_{min} = \varepsilon_{max}^{-1} = \sqrt{1 - \|[N_s \quad M_s]\|_{\infty}^2} = \sqrt{1 + \rho(XZ)} \quad (7)$$

Where: ε is an uncertainty boundary, called stability margin, ρ is the spectral radius (maximum eigenvalues), Z and X are the solutions of the Riccati equations simultaneously. These equations are so-called generalized control algebraic Riccati equation (GCARE) and generalized filter algebraic Riccati equation (GFARE) which can be written as follows [1]:

$$(A - BS^{-1}D^T C)Z + Z(A - BS^{-1}D^T C)^T - ZC^T R^{-1} CZ + BS^{-1}B^T = 0 \quad (8)$$

$$(A - BS^{-1}D^T C)X + X(A - BS^{-1}D^T C)^T - XBS^{-1}X + C^T R^{-1} C = 0 \quad (9)$$

Where $S = I + D^T D$ and $R = I + DD^T$

The controller which guarantees that:

$$\left\| \begin{bmatrix} K \\ I \end{bmatrix} (I - G_s)^{-1} M^{-1} \right\|_{\infty} < \gamma \quad (10)$$

is given by

$$K \approx \begin{bmatrix} K_{11} & K_{12} \\ K_{21} & K_{22} \end{bmatrix} \quad (11)$$

Where $K_{11} = A + BF + \gamma^2(L^T)^{-1}ZC^T(C + DF)$, $K_{12} = \gamma^2(L^T)^{-1}ZC^T$, $K_{21} = B^T X$, $K_{22} = -D^T$, $F = -S^{-1}(D^T C + B^T X)$, $L = (1 - \gamma^2)I + XZ$, and (A, B, C, D) are the minimum realization of the shaped plant G_s .

6. Controller Order Reduction

It is well-known that the robust control produces a high order controller compared to classical control. Several approaches are available for reducing the high order controller for instance; balanced truncation, balanced residualization and optimal Hankel norm approximation. Balanced truncation and balanced residualization approaches are convenient for removing the high frequency or fast modes of a state space realization [4], while an optimal Hankel norm approximation approach is used to remove the unobservable and/or uncontrollable modes [3]. Here the optimal Hankel norm approximation approach is selected to bound the additive error. The Hankel singular values, named after Hermann Hankel, provide a measure of energy for each state in the system. They are the basis for balanced model reduction, in which high energy states are retained while low energy states are discarded. The reduced model retains the important features of the original model [5]. For this paper the optimal Hankel norm approximation is selected.

7. Case Study: Aircraft Longitudinal Autopilot

This section illustrates the use to tune the longitudinal autopilot for an Aerosonde UAV flying at speed 23 /s and altitude 200 m. further, more information can be found in [8]. The aircraft model is fairly conventional and is given by:

$$\begin{bmatrix} \delta_e \\ \delta_r \end{bmatrix} = \begin{bmatrix} -0.2197 & 0.6002 & -1.4884 & -9.7965 \\ -0.5820 & -4.1201 & 22.4025 & -0.6461 \\ 0.4823 & -4.5281 & -4.7508 & 0 \\ 0 & 0 & 1.0000 & 0 \end{bmatrix} \begin{bmatrix} u \\ w \\ q \\ \theta \end{bmatrix} + \begin{bmatrix} 0.3246 & 0 \\ -2.1518 & 0 \\ -29.8191 & 0 \\ 0 & 0 \end{bmatrix} \begin{bmatrix} \delta_e \\ \delta_r \end{bmatrix} \quad (12)$$

the first step is to determine the desired loop shape which represents the specifications. The determination of the desired loop shape is an iterative process. The loop shape found to realize the specifications has the following transfer function [6]:

$$G_d = \frac{(2.8s + 0.3)}{(s + 0.05)^2} \quad (13)$$

The singular value of the desired loop shape is shown in Figure (6). The accuracy with which the control design matches the target desired loop is depicted with the dotted lines around the desired loop shape.

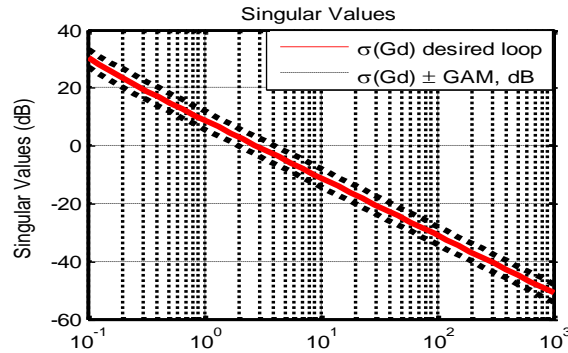


Fig. 6: SV shape of target desired.

The linear time invariant robust controller is found by shaping the central controller with shaping function. The state space form of the robust controller is obtained in equation (13).

The designed robust controller is optimally shaped and fitted the open loop frequency response of the plant to match as closely as possible a desired loop shape G_Δ as shown in Figure (7). The slope of the plant loop shape is increased at low frequency range so as to reduce the high frequency gain for good noise attenuation. The sensitivity function S and complementary sensitivity function T of the closed loop system is the in Figure (8). It is clear that design requirements for the disturbance rejection and noise attenuation are satisfied. The LSDP controller K ensures a stability margin of $\varepsilon = 0.6957$ or $\gamma = 1.4375$. This is a good level with respect to the robust stability, because a design is usually considered successful if $\varepsilon \geq 0.25$ or $\gamma \leq 4$ [1].

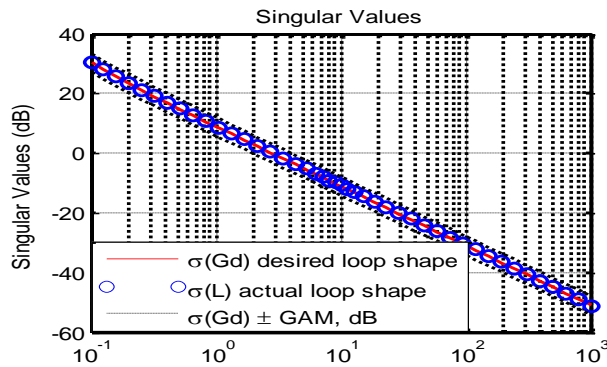


Fig. 7: Fitting open-loop SV into desired loop.

The frequency response of system is shown in the figure (9). The gain margin is modified from ∞ into 65 [dB], the phase margin modified from -81.2107 into 88.6861 [deg], and the bandwidth is modified from 0.9677 into 2.8637 [rad/s]. The controller order is reduced from ninth-order system, equation (13), to a third-order system by using Hankel norm approximation technique.

$$A_K = \begin{bmatrix} -3.793 & -568.4 & -1.211e+006 & -9.685e+005 & -2.026e+006 & -5.576e-016 & 5.628e-013 & 2.015e-013 & 1.296e-014 \\ 5.419e-022 & -8192 & -1.678e+007 & -1.342e+007 & -2.807e+007 & -1.091e-014 & 7.995e-012 & 3.317e-012 & 5.906e-014 \\ -1.084e-019 & 1 & 3.633e-012 & 0.04661 & 0.0975 & 1.955e-017 & -1.793e-015 & -8.933e-016 & -5.38e-017 \\ 0 & 0 & 0 & -0.05 & 0.1195 & -4.382e-023 & -1.713e-021 & 1.153e-021 & 1.51e-022 \\ 0 & 0 & 0 & 0 & -0.05 & -0.1219 & 4.337 & 1.655 & -0.05038 \\ 0 & 0 & 0 & 0 & 0 & -0.1568 & 10.13 & 4.513 & -0.1352 \\ 0 & 0 & 0 & 0 & 0 & 10.12 & -2270 & -1834 & 49.55 \\ 0 & 0 & 0 & 0 & 0 & -4.513 & 1834 & -5922 & 178.6 \\ 0 & 0 & 0 & 0 & 0 & 0.1352 & -49.55 & 178.6 & -5.402 \end{bmatrix} \quad B_K = \begin{bmatrix} -1.012e-013 \\ 1.653e-015 \\ -3.098e-016 \\ -3.001e-021 \\ 1.715 \\ 0.07283 \\ -2.592 \\ 0.9893 \\ -0.03011 \end{bmatrix} \quad (13)$$

$$D_K = [1.137e-013] \quad C_K = [0.1519 \quad -274.6 \quad -5.626e+005 \quad -4.501e+005 \quad -9.415e+005 \quad -6.214e-016 \quad 3.235e-013 \quad 1.203e-013 \quad 9.222e-015]$$

The Hankel singular value plot of the LSDP controller is shown in Figure (10). It showed that the controller K has most of its energy stored in states 1 through 3. It is expected that these states preserve most of the dynamic response of the system.

Starting from the first-order, the loop shape of the reduced-order controller is compared with the full-order one as shown in Figure (11). From the result, the following observations can be stated:

- The first-order controller response is not close to the full-order shape up to about 2950 [rad/s].
- The second-order controller response is not close to the full-order shape up to about 60 [rad/s].
- The third-order controller response is close to the full-order controller at all.

Therefore, the controller is reduced to the third-order, for which the state space form is as follows:

$$A_{K_r} = \begin{bmatrix} -8198 & -4102 & -38 \\ 4102 & -0.0034 & -0.02528 \\ -38 & 0.0260 & -3.215 \end{bmatrix} \quad B_{K_r} = [-1271 \quad 0.8183 \quad -2.987]^T \quad (14)$$

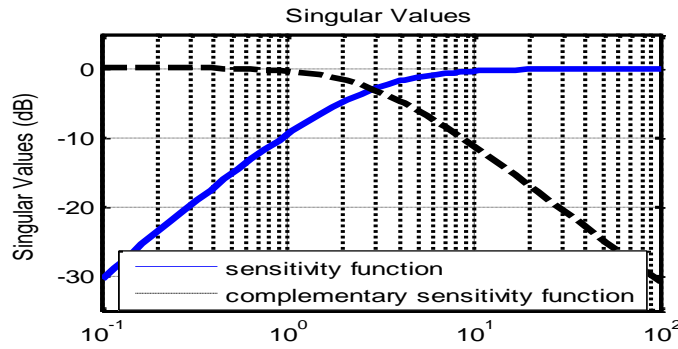


Fig. 8: S and T shape .

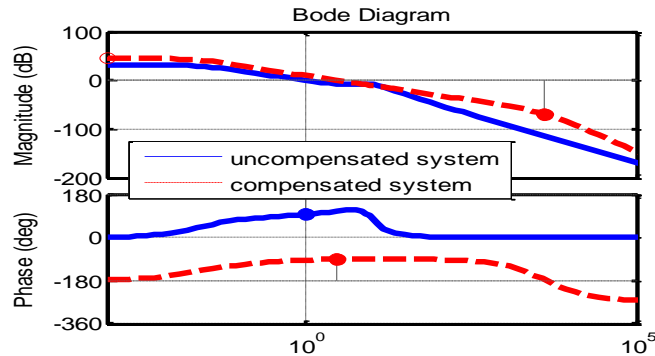


Fig. 9: Bode diagram.

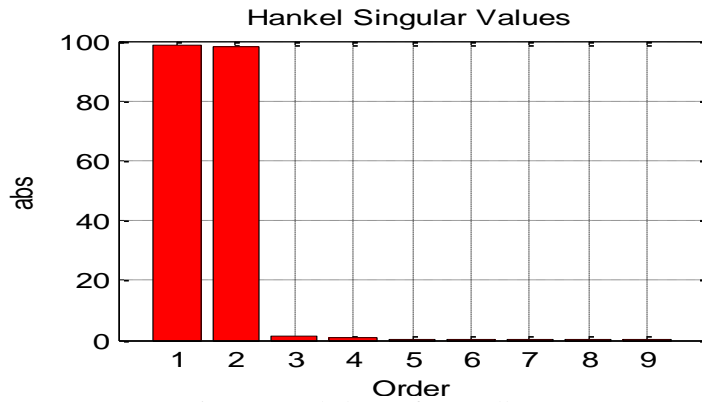


Fig. 10: Hankel SV of controller.

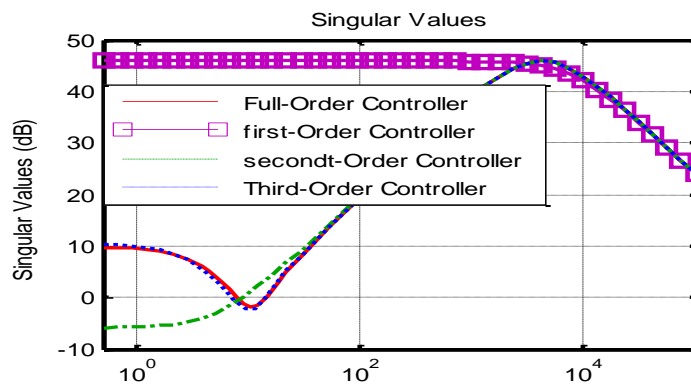


Fig. 11: Loop shape of full- and reduced order controller.

8. Controllers Comparison

Referring to a previous work which can be found in [6] and [7], a flight controller was designed for the same system utilising the classical technique. The design carried out using two schemes of controller (SDOF and the TDOF). For the SDOF scheme, a controller was designed using Z-N tuning first. Then its parameters were taken as initial guess and optimized using GA optimization under a acceptable of specifications. In order to improve the disturbance rejection properties while maintaining a good tracking criteria, a TDOF controller was designed. The results can be shown in figures (12), (13), (14), (15) and (16). It is clearly that for the classical controllers: the TDOF controller reveals its superiority to the SDOF controller in terms of performance and stability requirements, but SDOF is smoother in disturbance rejection. Unfortunately, all of classical controllers are sensitive to measurement noise, figure (16). Bearing this situation in mind, the robust controller is designed using H_∞ LSDP. Alongside, the comparison is made between classical and robust control in terms of nominal performance and robust stability. The nominal performance includes: speed of the system response and overshoot, while the robust stability includes: disturbance rejection, noise attenuation, unmodeled dynamics, and control effort. The result of comparison can be found in the same above figures. It reveals that the superiority of the robust control over the classical one in terms of stability requirements while maintaining equivalent level of performance as well as the classical.

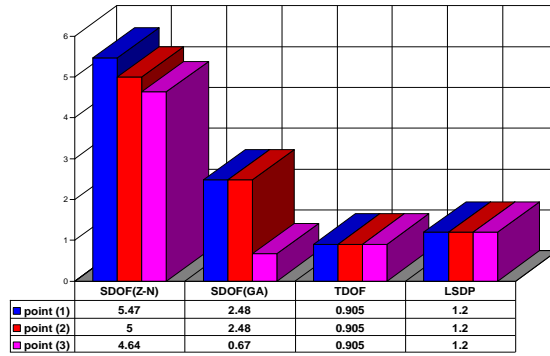


Fig. 12: Settling Time.

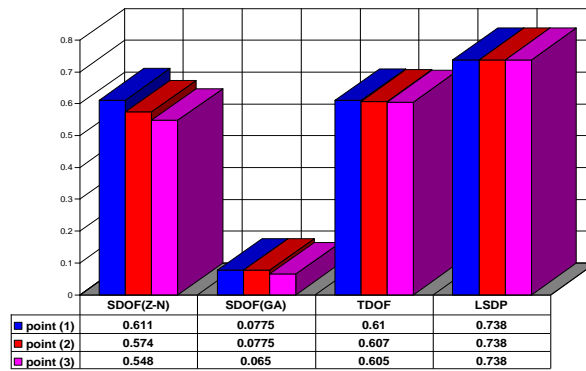


Fig. 13: Rise Time.

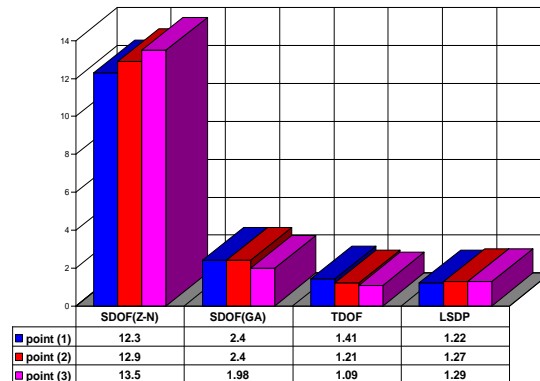


Fig. 14: Maximum Overshoot (%).

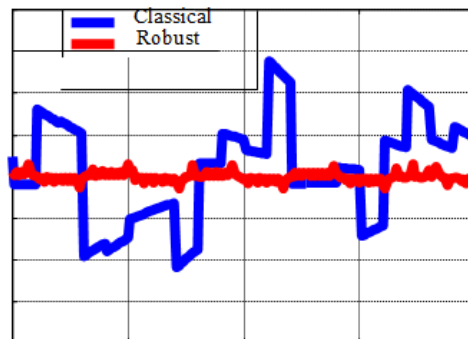


Fig. 15: Control effort.

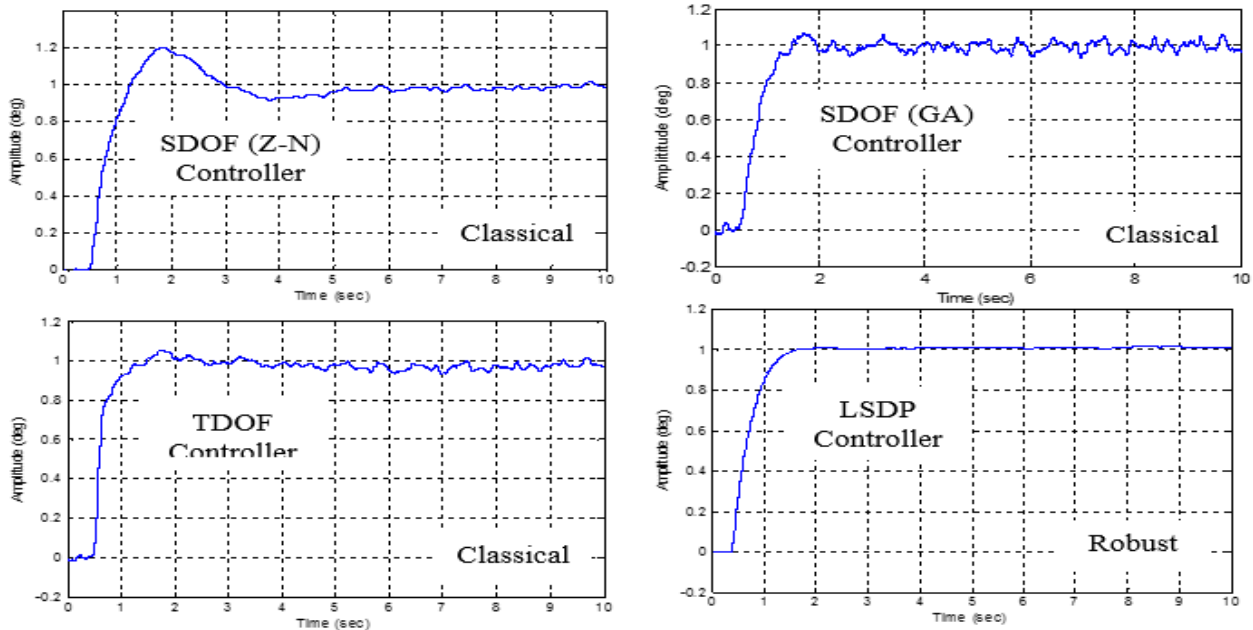


Fig. 16: System response to white noise and reference.

9. Conclusions

The design of robust controller for longitudinal dynamics is presented. The design carried out using the H_∞ loop shaping design procedure (LSDP). Then, the controller order reduction is performed. A maximum evaluation is successfully made in linear simulation for singular values as an ultimate test of the final reduced-order controller. The robust controller is then compared with the classical ones in terms of disturbance rejection, noise attenuation, unmodeled dynamics, and control effort. When comparing the two approaches classical and robust in terms of performance and stability aspect it is clearly that the robust control realized advantages over the classical control.

Nomenclature:

A, B, C, D	matrices used in the state space description
SDOF	single degree of freedom
TDOF	two degree of freedom
Z-N	Ziegler Nichol
GA	genetic algorithm
LSDP	loop shaping design procedure

References:

- [1] Salah I. AlSwailem, "Application of Robust Control in Unmanned Vehicle Flight Control System Design," Ph.D. Thesis, Cranfield, England, 2004.
- [2] G. J. Balas, A. K. Packard, M. G. Safonov and R. Y. Chiang, "Next generation of tools for robust control," *Proc. American Control Conf.*, Boston MA, 2004.
- [3] D.-W. Gu, P. H. Petkov and M. M. Konstantinov, *Robust Control Design with MATLAB*. Springer.
- [4] S. Skogestad and I. Poastlewaite, *Multivariable Feedback Control Analysis and Design*, 2nd ed. Wily, 2005.
- [5] *Robust Control Toolbox*, Version 5.3, (R2015a).
- [6] Eng. E. G. Hamdi, "UAV Robust Flight Control Systems," M. S. Thesis, MTC, Cairo, 2008.
- [7] Elfatih G. Hamdi, Ahmed M. Youssef, and Gamal A. Elsheikh, "UAV Classical Flight Control Systems", *6th International Conference on Electrical Engineering*, MTC, Cairo, 2008.